Spectrum of *HNF1A* Somatic Mutations in Hepatocellular Adenoma Differs From That in Patients With MODY3 and Suggests Genotoxic Damage

Emmanuelle Jeannot,[1,2] Lucille Mellottee,[1] Paulette Bioulac-Sage,[3] Charles Balabaud,[3] Jean-Yves Scoazec,[4] Jeanne Tran Van Nhieu,[5] Yannick Bacq,[6] Sophie Michalak,[7] David Buob,[8] Groupe d'étude Génétique des Tumeurs Hépatiques (INSERM Network), Pierre Laurent-Puig,[9] Ivan Rusyn,[2] and Jessica Zucman-Rossi[1]

OBJECTIVE—Maturity onset diabetes of the young type 3 (MODY3) is a consequence of heterozygous germline mutation in *HNF1A*. A subtype of hepatocellular adenoma (HCA) is also caused by biallelic somatic *HNF1A* mutations (H-HCA), and rare HCA may be related to MODY3. To better understand a relationship between the development of MODY3 and HCA, we compared both germline and somatic spectra of *HNF1A* mutations.

RESEARCH DESIGN AND METHODS—We compared 151 somatic *HNF1A* mutations in HCA with 364 germline mutations described in MODY3. We searched for genotoxic and oxidative stress features in HCA and surrounding liver tissue.

RESULTS—A spectrum of *HNF1A* somatic mutations significantly differed from the germline changes in MODY3. In HCA, we identified a specific hot spot at codon 206, nonsense and frameshift mutations mainly in the NH_2-terminal part, and almost all amino acid substitutions were restricted to the POU-H domain. The high frequency of G-to-T tranversions, predominantly found on the nontranscribed DNA strand, suggested a genotoxic mechanism. However, no features of oxidative stress were observed in the nontumor liver tissue. Finally, in a few MODY3 patients with *HNF1A* germline mutation leading to amino acid substitutions outside the POU-H domain, we identified a different subtype of HCA either with a gp130 and/or *CTNNB1* activating mutation.

CONCLUSIONS—Germline *HNF1A* mutations could be associated with different molecular subtypes of HCA. H-HCA showed mutations profoundly inactivating hepatocyte nuclear factor-1α function; they are associated with a genotoxic signature suggesting a specific toxicant exposure that could be associated with genetic predisposition. ***Diabetes*** **59:1836–1844, 2010**

From [1]Institut National de la Santé et de la Recherche Médicale, U674, Génomique Fonctionnelle des Tumeurs Solides; Université Paris Descartes, Paris, France; the [2]Department of Environmental Sciences and Engineering, University of North Carolina, Chapel Hill, North Carolina, USA; the [3]Institut National de la Santé et de la Recherche Médicale, U889, Université Bordeaux 2, IFR66, Centre Hospitalier Universitaire Bordeaux, Hôpital Pellegrin, Bordeaux, France; [4]Hôpital Edouard Herriot, Lyon, France; the [5]Assistance Publique-Hôpitaux de Paris, Pathology Department, Hôpital Henri Mondor, Créteil, France; [6]Hôpital Trousseau, Centre Hospitalier Régional et Universitaire de Tours, Tours, France; [7]Centre Hospitalier Universitaire, Pathology Department, Angers, France; [8]Pôle Pathologie, Centre de Biologie Pathologie, Centre Hospitalier Régional et Universitaire de Lille, Lille, France; and the [9]Institut National de la Santé et de la Recherche Médicale, U775; Université Paris Descartes, Paris, France.

Corresponding author: Jessica Zucman-Rossi, zucman@cephb.fr.

Received 14 December 2009 and accepted 31 March 2010. Published ahead of print at http://diabetes.diabetesjournals.org on 14 April 2010. DOI: 10.2337/db09-1819.

Hepatocellular adenoma (HCA) is a rare, benign, liver tumor frequently associated with oral contraception (1,2). HCA usually manifests as a single tumor, but in some cases, several adenomas are detected in the same patient; when >10 nodules are identified in the liver it is called liver adenomatosis (3). Recently, by the analysis of a large series of patients with HCAs, we established a new molecular classification of these tumors. Adenomas were classified according to the genotype of the tumors, such as the finding of mutations in *HNF1A*, in *CTNNB1*-activating β-catenin and/or in the interleukin-6 transducer of signal (*IL6ST*) activating gp130 (4–8). Close relationships were found between the molecular subgroups defined by genotype and the clinical/pathologic findings (4,8). Particularly, *HNF1A*-mutated HCAs (H-HCAs) represent a homogeneous group of tumors with marked and diffuse steatosis without significant inflammation or cytologic abnormalities (4,8). In these tumors, downregulation of *LFABP1* (encoding liver fatty acid-binding protein), a gene positively regulated by *HNF1A*, may contribute to this phenotype through impaired fatty acid trafficking together with an aberrant promotion of lipogenesis (9).

Heterozygous germline mutations of *HNF1A* are also the cause of maturity onset diabetes of the young type 3 (MODY3), a monogenic form of noninsulin-dependent diabetes (10). A few cases of familial liver adenomatosis were identified in patients with MODY3 (5,11,12). In these patients, one *HNF1A* mutation was germline, whereas the other was somatic and occurred only in tumor cells. In most of these families, penetrance of adenomatosis is low, and in one of them, we identified a *CYP1B1* heterozygous germline mutation as a genetic event associated with the occurrence of HCA (13). Occurrence of HCA in individuals with MODY3 is rare, and the biologic underpinnings of this phenomenon remain to be explained.

The *HNF1A* gene (previously called *TCF1*) codes for the transcription factor hepatocyte nuclear factor (HNF)-1α. HNF1α protein recognizes specific palindromic nucleotide DNA sequences and interacts with DNA as either a homodimer or a heterodimer with HNF1β (14,15). HNF1α plays an important role by regulating the expression of many key liver genes involved in glucidic metabolism, lipidic transport, and detoxication (16–19). HNF1α is a protein composed of three functional domains (Fig. 1*A*): a dimerization domain (amino acids 1–32), a DNA-binding domain (91–276), and a carboxyl-terminal transactivation

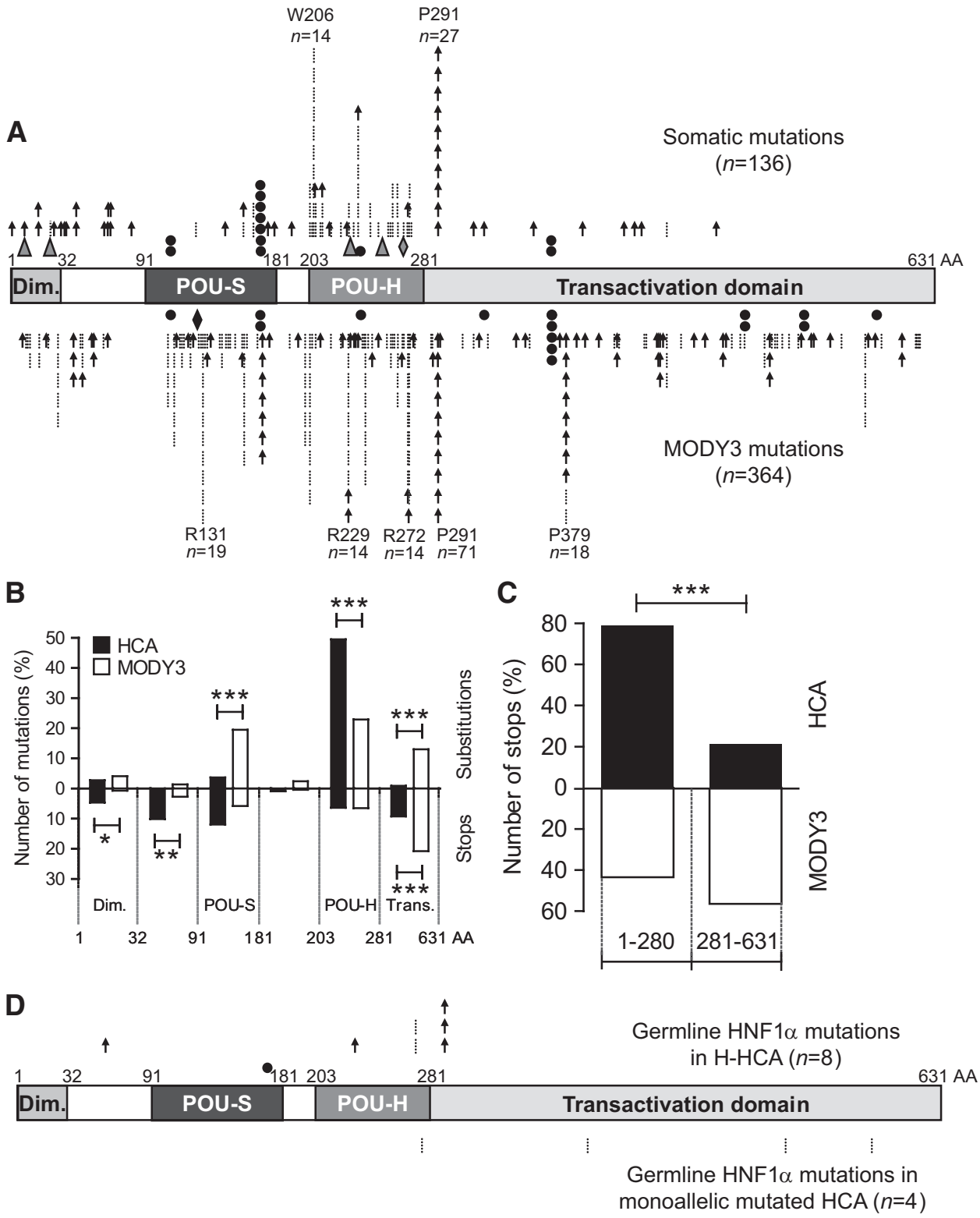

FIG. 1. ***A*: Spectrum of 136 somatic *HNF1A* mutations observed in 75 HCA samples (*top*) and in 364 MODY3 individuals (*bottom*) (data from Ellard and Colclough [25]). Each arrow indicates a point mutation leading to a frameshift or a stop codon. Each bar indicates a point mutation leading to an amino acid substitution. ▲, in-frame deletion; ♦, in-frame duplication; ●, mutation in splicing site. *B*: Comparison of the number of substitutions and stops in different HNF1α domains. HCA (■) and MODY3 (□) histograms represent the percentage of total mutations observed in each domain; substitutions and stops are represented in the upper part and the lower part, respectively. Significant differences between HCA and MODY3 individuals are indicated: *0.05 > *P* > 0.01; **0.01 > *P* > 0.001; ****P* < 0.001. *C*: Comparison of the number of stops in the transactivation domain (281–631) vs. the rest of the protein observed in individuals with HCA (■) and MODY3 (□). ***Significant difference (*P* < 0.001) between the two populations. *D*: Spectrum of eight germline *HNF1A* mutations identified in H-HCA (*top*) and five germline *HNF1A* mutations identified in monoallelic mutated HCA (*bottom*). AA, amino acids.**

domain (281–631). The DNA-binding domain is composed of a POU-S domain (91–181) and an atypical homeodomain POU-H (203–280) formed by 3 α-helices and an insertion of 21 amino acids between Hα2 and Hα3 (20). Most of the *HNF1A* mutations observed in patients with HCA and MODY3 are predicted to inactivate the protein function (5,8,10,21,22). Correlations have been identified linking the position of the mutations in *HNF1A* and the age of diabetes onset, a phenomenon that can be explained by the specific isoforms that are expressed in the fetal or adult pancreas (21,22). Based on these data, we can hypothesize that not all mutations demonstrate the same effect on the HNF1α function.

In this study, we hypothesized that rare occurrence of HCA in MODY3 may be caused by differences in the somatic and germline spectra of mutations, both concerning their origin and their functional consequences. To test this hypothesis, we compared the spectrum of *HNF1A* mutations identified in HCA with that identified in MODY3. Then, taking advantage of working on human liver tissues with mutations occurring under their endogenous promoter, we evaluated the consequences of several *HNF1α* mutants at the mRNA expression and protein levels. We also investigated the potential mechanism of *HNF1A* mutagenesis by *1*) comparing our observations with studies of a known genotoxic agent and *2*) assessing the level of oxidative stress in the liver.

RESEARCH DESIGN AND METHODS

A group of 14 university hospitals participated in this study and 72 patients were recruited between 1992 and 2006. Individuals with confirmed *HNF1A*-mutated HCA who underwent curative resection of the tumor(s) were eligible for inclusion in this study. The mean age of the patients was 37.5 years (ranging from 14 to 66 years), and there were only seven male patients. Among the women studied, 71% (34 of 48) had a history of oral contraception use, and 17 patients were missing this data. There were 89 *HNF1A*-mutated HCA samples from 72 patients, although 44 samples had been reported previously (8). In 10 patients with multiple and sporadic tumors, several nodules were genotyped. For each patient, different somatic *HNF1A* mutations were observed in the genotyped nodules. For all patients, a representative part of the HCA nodule, as well as of the nontumor liver when it was available, was immediately frozen in liquid nitrogen and stored at −80°C until used for molecular studies. The study was conducted in accordance with French law and institutional ethical guidelines. The Ethical Committee of the Saint-Louis Hospital (Paris, France) approved the overall design of the study.

Mutation screening. In all 89 tumors, we sequenced the *HNF1A* gene using direct sequencing of the exons on genomic DNA or RT-PCR to identify mutation, as previously described (5). All identified mutations (Tables 1 and 2) were confirmed by two independent PCR amplifications of genomic DNA from tumor, and corresponding nontumor tissues were systematically sequenced to search for germline mutations. In samples with mutations affecting splicing sites, we characterized the transcripts by sequence analysis of the mRNA transcripts. In 37 H-HCA, the coding exons of *MYH* (exons 1–16) and *OGG1* (exons 1–7) were screened for mutations by direct sequencing of PCR products. Oligonucleotides used for all PCR reactions and experimental conditions are listed in supplementary Tables 1 and 2 available in an online appendix at http://care.diabetesjournals.org/cgi/content/full/db09-1819/DC1. Allelic frequency of an *OGG1* polymorphism observed in H-HCA was compared with those obtained in a control group of non-*HNF1A*-mutated hepatocellular tumors (58 samples) as previously described (13) and presented in supplementary Table 3 (available in an online appendix).

Quantitative RT-PCR. Total RNA was extracted using the RNeasy kit (Qiagen, Valencia, CA) from all frozen samples of available HCA and nontumor liver tissues. RNA isolated from 16 H-HCA and 24 nontumor tissue samples was deemed to be of acceptable quality for quantitative RT-PCR experiments (23). Specific assays for *MYH* (Hs01014866_g1), *OGG1* (Hs00213454m1), *APE1* (Hs00172396_m1), *POLβ* (Hs00160263_m1), *FABP1* (Hs00155026_m1), *UGT2B7* (Hs00426592_m1), and *R18S* (rRNA, Hs99999901_s1) were obtained from Applied Biosystems (Foster City, CA). The relative amount of target gene mRNAs was determined using the $2^{-\Delta\Delta C_T}$ method (24). The values obtained for *FABP1* and *UGT2B7* were expressed as the *n*-fold ratio of the gene expression in a tested sample as compared with the mean of 11 nontumor tissues. Only six nontumor tissues from patients with a H-HCA were used with the *MYH*, *OGG1*, *APE1*, and *POLβ* assays. The values obtained were compared with the mean of seven nontumor tissues from patients with a non-*HNF1A*–mutated HCA.

Western blotting. Western blot analyses were performed as described (9) using two primary goat polyclonal anti-HNF1α antibodies (Santa Cruz Biotechnology), one detecting the amino terminus, and the other detecting the carboxy terminus of the protein (SC-6548 and SC-6547, respectively), used at the dilution 1:500.

Determination of reduced and total glutathione levels. Approximatively 50 mg of frozen nontumor liver tissues were homogenized in 5% 5-sulfosalicylic acid. After centrifugation at 8,000*g* for 10 min, the supernatant was assessed for reduced and total glutathione content with an ApoGSH Glutathione Colorimetric Assay Kit (BioVision, Mountain View, CA), following the manufacturer's protocol.

Immunohistochemistry. Formalin-fixed, paraffin-embedded sections (5 μm) were mounted on glass slides. Sections were deparaffinized in xylene, rehydrated in a series of graded alcohol concentrations, and placed in PBS with 0.1% Tween 20. Immunostaining was performed using a DAKO EnVision System horseradish peroxidase (Dako Cytomation, Carpinteria, CA) kit using primary antibody (1:2,000 dilution in PBS containing 1% BSA, incubated overnight at 4°C) against 4-hydroxynonenal protein adducts (Alpha Diagnostics, San Antonio, TX). Slides were counterstained with hematoxylin and mounted with glass coverslips.

Statistical analysis. Statistical analysis was performed using GraphPad Prism software (version 4, GraphPad Software, San Diego, CA). Allelic frequencies of the *OGG1* polymorphism in H-HCA and the group control were compared using contingency tables with a Fisher exact test.

RESULTS

Spectrum of *HNF1A* mutations in HCA differs from that in MODY3. Among 89 HCA samples with *HNF1A* alteration, mutations and deletion were biallelic in 84 (94%) samples. To further analyze the spectrum of *HNF1A* mutations, we included 151 *HNF1A* alterations with a firm somatic origin identified in 75 different HCAs; in contrast, all samples with a proven or highly suspected germline mutation were excluded from this first analysis (Fig. 1*A*).

Among 151 *HNF1A* somatic alterations, 90% were point mutations, and the remaining 10% (15 of 151) were gene deletions as evidenced by the loss of heterozygosity at a *HNF1A* single nucleotide polymorphism(s) compared with the corresponding nontumor tissues. Among the mutations, 57 were missense, 62 were frameshift and nonsense, and 12 were mutations affecting a splicing site. The five remaining mutations were small in-frame deletions or duplication (Fig. 1*A*, Table 1).

Next, we compared the spectrum of somatic *HNF1A* mutations identified in HCA with 364 germline mutations previously described in individuals with MODY3 without HCA (Fig. 1*A*, lower panel, supplementary Table 4, available in an online appendix) and by Ellard and Colclough (25). In both HCA and MODY3, a hotspot mutation at codon 291 was present, whereas a hotspot mutation at codon 206 was specifically identified in HCA (Fig. 1*A*). As previously reported, codon 291 mutation is located in a polyC-8 tract, whereas codon 206 mutation is not located in a repeated sequence motif. Because codon 291 mutations represented 20% of the mutations in both spectra, we did not include them in the following analysis. There was no significant difference ($P = 0.16$) in the proportion of missense and truncating (frameshift, nonsense, and mutations affecting a splicing site) mutations in MODY3 and HCA spectra. Thus, there were 63 and 55% of missense mutations in MODY3 and HCA, respectively, and 37 and 45% of truncating mutations in MODY3 and HCA, respectively. In contrast, the distribution of the mutations was significantly different in HCA compared with the MODY3

TABLE 1
Biallelic *HNF1*A mutations identified in HCA

No.	Tumor tissue	
	Allele 1	Allele 2
Somatic origin		
154*	872–873insC, P291fs†	749A>C, Q250P
196*	379 A>T, N127Y	495G>T, W165C
357*‡	IVS2 + 1G>A, W165X†	618G>T, W206C
358*‡	617G>T, W206L	872–884del, P291fs
368*‡	710A>G, N237S	LOH
369*‡	436–437delC, Q146fs	LOH
370*‡	872–873insC, P291fs†	803T>G, F268C
371*‡	617G>T, W206L	730A>G, R244G
373*‡	82C>T, Q28X†	LOH
380‡	196G>T, E66X	779C>T, T260M†
383‡	493T>A, W165R	1340C>T, P447L†
384*	17–35insT, 7–12del	26–32del, Q9fs
385*‡	817A>G, K273E	LOH
461‡	872–873insC, P291fs†	872–873delC, P291fs†
462‡	632A>C, Q211P	670C>G, P224A
463	632A>C, Q211P	617G>T, W206L
464‡	71–82del, A25-Q28del	747–764del, Q250-G255del
474‡	617G>T, W206L	LOH
476‡	232–245dup, T81fs	1,288–1289delG, G430fs
496	872–873insC, P291fs†	796–798dup, N266dup
508‡	77T>A, L26Q	872–873delC, P291fs†
516‡	185–194del, N62fs	788G>A, R263H†
532‡	198–202del, T67fs	618G>T, W206C
535‡	617G>T, W206L	872–873insC, P291fs†
539‡	686G>A, R229Q†	775G>C, V259L
540‡	618G>T, W206C	LOH
546‡	1 A>G, M1X	620G>A, G207D†
575‡	IVS2 + 1 del13	956–957delG, G319fs
578	788 G>T, R263L†	IVS5 + 1 G>T
579	132–156del, D45fs	872–873insC, P291fs†
583‡	811–818del, R271fs	815G>A, R272H†
584‡	607C>T, R203C†	710A>G, N237S
591‡	787C>T, R263S	LOH
592‡	526C>T, Q176X†	IVS5–2 A>G†
621	711 T>G, N237K	872–873insC, P291fs†
633	872–873insC, P291fs†	650–654del, A217fs
635	618G>C, W206C	872–873insC, P291fs†
682‡	197–198insA, T67fs	872–873insC, P291fs†
683	695–697del, V233del	613 A>C, K205Q†
687‡	814C>A, R272S†	LOH
688	710A>G, N237S	LOH
689	IVS1 + 2delTA	56 C>A, S19X
690	IVS1–2 A>T	872–873insC, P291fs†
694‡	682G>T, E228X	IVS2–2 A>G
695	105–144delinsTTC, P35fs	IVS2–2 A>G
696‡	872–873insC, P291fs†	1168G>T, E390X
699‡	685C>G, R229G	710–711insA, N237fs
705‡	618G>T, W206C	631C>T, Q211X
749	618G>T, W206C	LOH
759	IVS2 + 1 G>A†	608G>T, R203L
761	617G>T, W206L	618–628del, W206fs
762	IVS2 + 1 G>A†	LOH
763	872–873insC, P291fs†	IVS2 + 1 G>A†
778	1,067–1073del7, L356fs	1441C>T, Q481X
785	108C>A, Y36X	570–577del, T191fs
806	618G>T, W206C	872–873insC, P291fs†
814	476G>A, R159Q†	872–873insC, P291fs†
815	779C>T, T260M†	872–873insC, P291fs†
816	872–873insC, P291fs†	IVS3 + 8, insAGT, dup637-IVS3 + 7
817	196G>T, E66X	711T>A, N237K

Continued on facing page

TABLE 1
Continued

No.	Tumor tissue	
	Allele 1	Allele 2
818	710A>G, N237S	872–873delC, P291fs†
829	695T>A, L232Q	931–932delGinsACCTA, A311fs
831	815G>A, R272H†	872–873insC, P291fs†
833	607C>T, R203C†	LOH
850	872–873insC, P291fs†	133–149del, D45fs
851	872–873delC, P291fs†	LOH
856	872–873delC, P291fs†	770A>C, N257T
957	730A>G, R244G	1,274–1275delC, T425fs
964	629C>T, S210F	LOH
971	620G>A, G207D†	872–873delC, P291fs†
972	618G>T, W206C	1,249–1250insT, G417fs
1,025	97–103del, P33fs	872–873insC, P291fs†
Germline origin (**allele 1**)		
340*‡	**685C>T, R229X**†	LOH
487‡	**814 C>A, R272S**†	LOH
509‡	**391C>T, R131W**†	872–873delC, P291fs†
514‡	**829–837del, F277-H279**	872–873insC, P291fs†
518‡	**164–168del, G55fs**†	LOH
523‡	**872–873insC, P291fs**†	LOH
590‡	**257–258delT, L86fs**	IVS2 + 1 G>T
965	**252–258del, I85fs**	815G>A, R272H†
Undetermined origin		
479‡	476–479del, R159Pfs	811C>T, R271W†
482‡	653 A>G, Y218C†	LOH
489‡	IVS1–2 A>T	1,072–1073delCins11, P358fs
548	IVS1–1 G>T	1,072–1073delCins11, P358fs
951	534–535insA, H179fs	779C>T, T260M†

Cases of HCA were previously described in *Bluteau et al. (5) or ‡Zucman-Rossi et al. (8). MODY3 mutations were previously described in †Ellard and Colclough (25) or Bellanné-Chantelot et al. (21). Case 535 has a third somatic mutation, 51–60delins6, S19fs. Boldface indicates allele 1. del, deletion; fs, frameshift; IVS, intervening sequence; LOH, loss of heterozygosity; ins, insertion; Nm, nonmutated.

spectrum. Although almost all of the missense mutations were restricted to the POU-H domain ($P < 0.001$) in HCA, they were distributed in all HNF1α domains in individuals with MODY3 (Fig. 1*B*). Also, in HCA, truncating mutations were localized predominantly in the first 280 amino acids ($P < 0.001$), whereas they were distributed equally between the first 280 amino acids and the transactivation domain in the individuals with MODY3 (Fig. 1*C*).

Germline *HNF1A* mutations are found in H-HCA or in other subtypes of adenomas. In a second step, we analyzed the distribution of the 13 germline *HNF1A* mutations identified in patients with adenomas. In eight patients, we identified a mutation of the second *HNF1A* allele in the corresponding tumor leading to a biallelic inactivation of HNF1α (Table 1). The corresponding germline mutations fit the distribution of the somatic *HNF1A* mutations: six of them were nonsense or frameshift occurring before codon 292, and the remaining two mutations were missense affecting codon 272, an amino acid found to be mutated by a somatic event (Fig. 1*D*). In contrast, in four HCA samples [372 (R583Q), 769 (T525S), 966 (L389V), and 998 (R278Q)], we observed a germline *HNF1A* mutation without alteration of the second *HNF1A* allele. All of these germline mutations were missense; three of them localized in the transactivation domain, and the last one was at the end of the POU-H domain. None of these mutations were described in the spectrum of somatic *HNF1A* mutations; however, three of them (R583Q, T525S, and L389V) have been previously reported in individuals with MODY3 (21,25). Thus, these four germline mutations did not fit the characteristic distribution of the somatic one. Moreover, the corresponding adenomas were classified in different molecular subgroups of HCA: one of them was β-catenin activated (case 372), two were inflammatory adenomas with or without a gp130 activating mutation (cases 769 and 966), and the last one remained unclassified (case 998).

TABLE 2
Germline *HNF1*A mutations in monoallelic mutated HCA

No.	Allele 1	Allele 2
372*†	1748G>A, R583Q‡	Nm
769	1573A>T, T525S§	Nm
966	1165T>G, L389V§	Nm
998	833G>A, R278Q	Nm

Cases of HCA were previously described in *Bluteau et al. (5) or ‡Zucman-Rossi et al. (8). MODY3 mutations were previously described in †Ellard and Colclough (25) or Bellanné-Chantelot et al. (21). Nm, nonmutated.

Functional consequences of *HNF1A* mutations in HCA. Most of the somatic mutations found in HCA are predicted to inactivate the protein because they are almost all biallelic and frequently nonsense or missense affecting the POU-H domain that is essential for DNA binding. We also analyzed the consequence of seven mutations that affected different splice sites. All of these mutations resulted in aberrant splicing, the outcome of which is either an aberrant protein with an early stop (Fig. 2*A*, *B*, and *D*), or a protein with an amino acid replacement and a deletion of five amino acids in the DNA-binding domain (Fig. 2*C*).

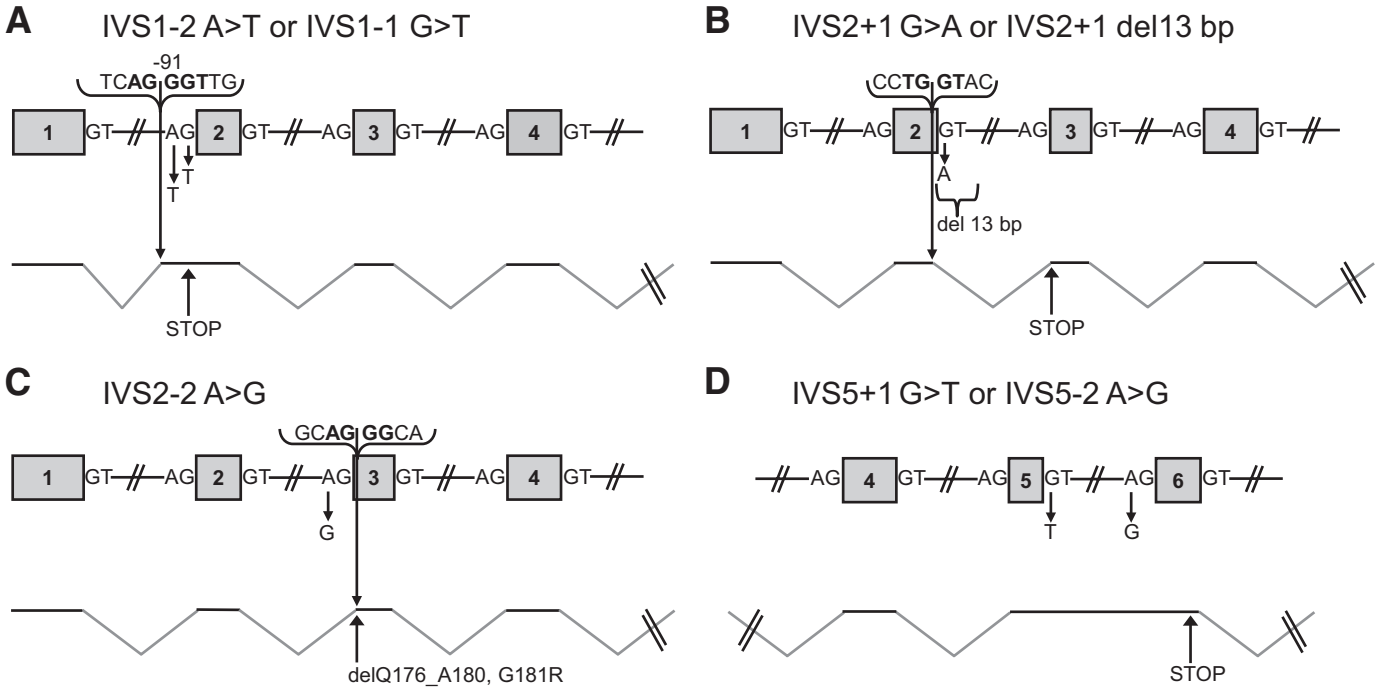

FIG. 2. Consequences of the mutations at different splice sites in *HNF1A*. *A*: IVS1–2 A>T or IVS1–1 G>T mutations. *B*: IVS2 + 1 G>A or IVS2 + 1 del 13 bp mutations. *C*: IVS2–2 A>G mutation. *D*: IVS5 + 1 G>T or IVS5–2 A>G mutations. del, deletion; ins, insertion; IVS, intervening sequence.

Then we assessed the protein level of mutant HNF1α in HCA and compared it with that in nontumor tissue. Samples with mutations leading to an early stop contained little detectable HNF1α protein (supplementary Fig. 1, available in an online appendix; samples identified with arrows and data on gradient migration, not shown). Additionally, some samples harboring missense mutations exhibited a dramatic increase in the expression of *HNF1α* compared with normal liver (supplementary Fig. 1).

The HNF1α transcription factor regulates expression of several key liver genes, including *UGT2B7* and *FABP1* (16,18). Indeed, a shutdown of mRNA expression for these target genes was observed in all patients with HCAs tested with biallelic *HNF1A* mutations, as previously reported (4). An effect of monoallelic HNF1α mutants on expression of *UGT2B7* and *FABP1* has not been previously examined in liver tissues. Our data show that monoallelic mutations did not affect expression of *FABP1* and *UGT2B7*, which is not in favor of a dominant-negative effect (Fig. 3). However, these results cannot completely exclude a subtle dosage effect or a low dominant effect.

***HNF1A* mutations in HCA are likely to arise due to a genotoxic event.** In contrast to other solid tumors, point mutations were much more frequent in HCA than were chromosome deletions. The latter were found in only 10% of the patients with HCAs. Among the point mutations in HCA, we analyzed the proportion of different *HNF1A* nucleotide changes and found that G-to-T transversions, accounting for 36% of the cases, were the most common type (Fig. 4*A*). Moreover, the distribution of nucleotide substitution subtypes in H-HCA was strikingly different from that in MODY3 (Fig. 4*B*) but very similar to a spectrum of mutations known to be induced by genotoxic events, that is, in *TP53*-mutated lung cancers in smokers (Fig. 4*C*) (26). In addition, when the *HNF1A* nucleotide substitutions were partitioned between the two DNA strands, we observed that G-to-T transversions were significantly more frequent on a nontranscribed strand ($P = 0.01$) (Fig. 4*D*). Taking these results together, we suggest that *HNF1A* somatic mutations showed a typical spectrum of mutations induced by the genotoxic exposure targeting a specific nucleotide sequence.

***HNF1A* spectrum of mutation is not related to measurable increase in oxidative stress in liver.** Because both direct DNA damage by an environmental agent and oxidative stress are known to result in G-to-T transversion mutations (27,28), we also assessed oxidative stress markers in nontumor liver from six patients with H-HCA and seven patients with non-*HNF1A*–mutated HCA (supplementary Fig. 2, available in an online appendix). We observed no difference in total or reduced glutathione content, expression of four base excision DNA repair

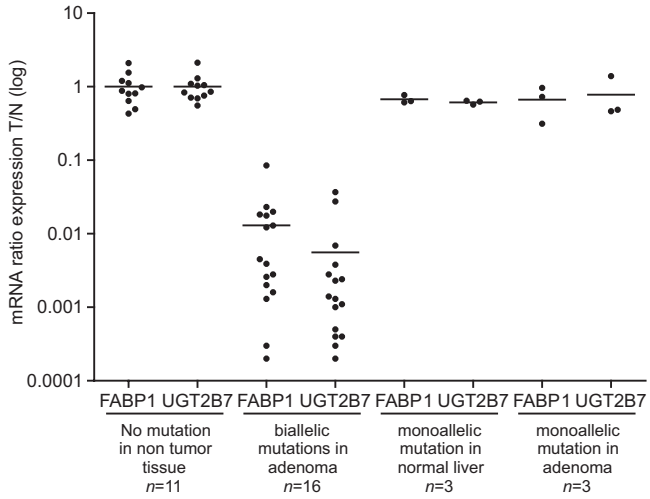

FIG. 3. Expression of *FABP1* and *UGT2B7* is abrogated in adenomas with *HNF1A* biallelic mutations. Mean levels of expression in each group is represented by a horizontal line.

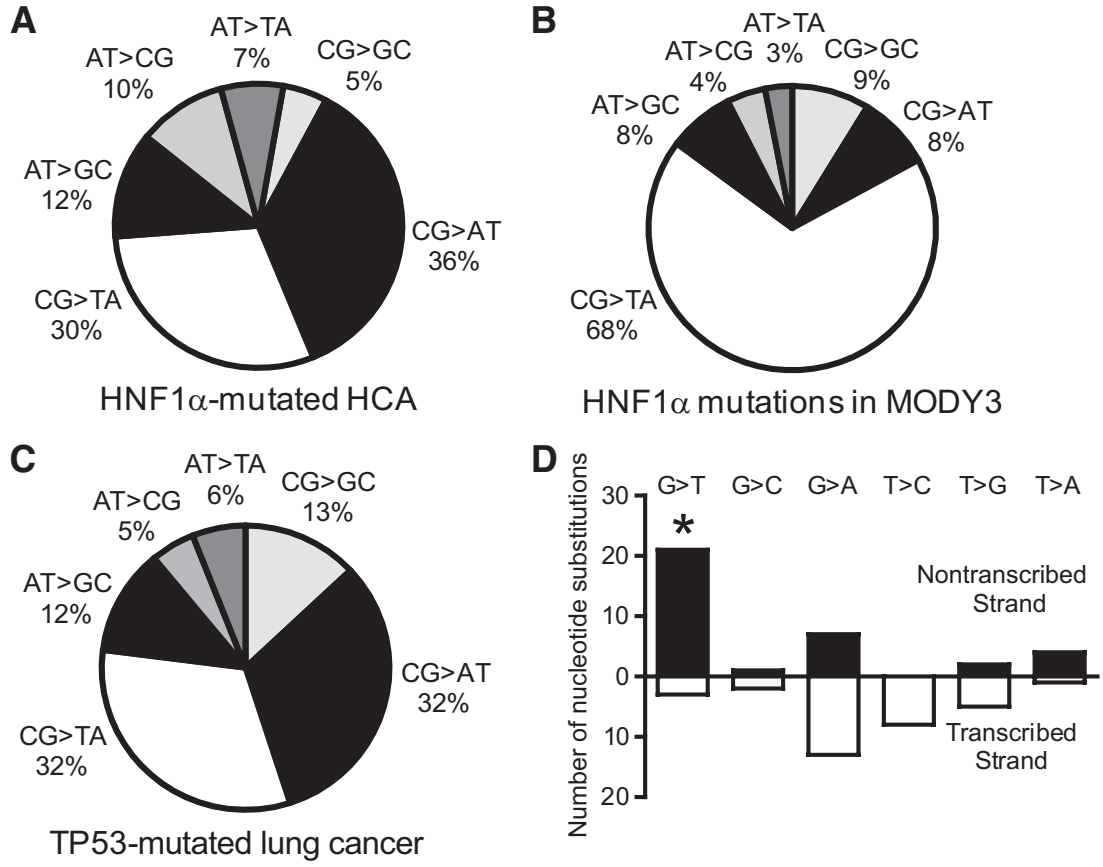

FIG. 4. Comparison of the mutation profiles in H-HCA (67 transversions and transitions, *A*), MODY3 (229 transversions and transitions, *B*), and *TP53*-mutated lung cancers (311 transversions and transitions, *C*) and smokers (26) (*D*). Repartitioning of transition and transversion mutations between the transcribed and the nontranscribed strands in H-HCA. Black and white histograms indicate the number of nucleotide substitutions on the nontranscribed and the transcribed strand, respectively. *Significant ($P = 0.01$) elevation in G-to-T transversions on the nontranscribed strand.

genes, markers of oxidative DNA damage (29), or 4-hydroxynonenal protein adducts, a marker of lipid peroxidation (supplementary Fig. 3), between these two groups. These data showed a lack of evidence for elevated oxidative stress in livers of patients with H-HCA as a potential source of DNA mutations.

In addition, it is possible that a large number of G-to-T transversions could be caused by inefficient repair of DNA damage due to mutations or polymorphisms in *MYH* and *OGG1*, genes involved in the repair of 8-hydroxyguanine (30–32). Thus, we sequenced *MYH* and *OGG1* DNA in 37 subjects with an *HNF1A*-mutated HCA, and no mutations were detected in either gene. A known functional polymorphism in *OGG1* (S326C) was detected in *HNF1A*-mutated HCA subjects, albeit there was no difference in the frequency of this polymorphism compared with that in control subjects (supplementary Table 3, available in an online appendix).

DISCUSSION

In this study we analyzed the spectrum of *HNF1A* mutations in HCA and showed a significant difference in pattern in comparison with individuals with MODY3, both at the nucleotide and amino acid levels. In HCA, location of the mutations is very restricted because almost all of the truncating mutations led to the loss of the transactivation domain and the missense mutations altered mainly the POU-H domain. When we take into account the two largest series of *HNF1A* screening in MODY3 (21,25), only 48% of the germline mutations (117 of 720 are missense mutations in POU-H, and 227 of 720 are truncating mutations localized in the first 291 amino acids) fit the features of the *HNF1A* somatic mutations. This observation suggests that only a part of *HNF1A* mutations that are associated with diabetes could predispose to the development of a H-HCA.

Previous analysis of the MODY3 mutations showed that the age at onset of diabetes is modulated according to the position of the mutation relative to the *HNF1A* isoforms: missense mutations located in exons 7 to 10 that affect only A or B isoforms of *HNF1A* are associated with the late onset of diabetes (21,22). Interestingly, these mutations are predicted to have a less severe effect on the HNF1α function and are not found in HCA. Similarly, we can hypothesize that frequent MODY3 missense mutations located outside the POU-H domain and mutations truncating HNF1α after codon 291 are possibly less inactivating than the mutations found in HCA. In contrast to MODY3, in HCA the lack of mutations leading to amino acid substitution in POU-S suggests that the POU-S and POU-H domains are functionally different. Chi et al. (20) found that the POU-S domain interacts with the POU-H domain in the recognition and binding on promoter sequences; however, the POU-S domain is not conserved in homeobox transcription factors outside the POU family. Thus, based on the profile of the *HNF1A* mutations that occur in HCA, it may be of interest to reanalyze clinical severity of the diabetes and putative associated phenotypes in patients with MODY3, taking into the account only

a premature stop before codon 291, missense restricted at POU-H, and mutations affecting splicing sites from exon 1 to 7.

Interestingly, among the five HCAs with a monoallelic germline *HNF1A* mutation, three of them were inflammatory. We previously noted that inflammatory adenomas are associated with obesity (4), and the present observation raised the question of an association with MODY3 and possibly with other subtypes of adenomas. We can hypothesize that according to the nature of their *HNF1A* germline mutation, patients with MODY3 could be at risk of different subtypes of HCA: mutations leading to a severe impaired HNF1α function predispose to the development of H-HCA, whereas germline mutation with a mild functional consequence could predispose to inflammatory or ß-catenin–activated HCAs without a familial context. In consideration of the high risk of malignant transformation of the β-catenin-activated HCA, this observation could have important clinical consequences.

Our analysis of the expression of mutant HNF1α proteins in liver tissue did not reveal a detectable level of truncated proteins, and most of the mutated proteins were not expressed. Moreover, mutations of both *HNF1A* alleles are required to observe a downregulation of the genes physiologically regulated by HNF1α. These observations suggest that if a dominant-negative effect exists, as suggested by the in vitro analyses for particular *HNF1A* mutants (15), it is not sufficient to shut down activity of HNF1α in vivo. Accordingly, other researchers (33,34), including Harries et al. (35) showed that *HNF1A* transcripts harboring a premature termination codon (PTC) were less expressed in lymphoblastoid cells than the normal allele resulting from a "nonsense-mediated mRNA decay," which detects and degrades the transcripts with a PTC to prevent the synthesis of truncated proteins. In the present study, we observed a decrease of mRNA expression for 16 of 21 different mutants leading to PTC (data not shown). Altogether, in hepatocytes, a dominant-negative effect of an HNF1α mutant is unlikely in vivo.

This study not only confirms, in a large series of adenomas, that the spectrum of *HNF1A* mutations in HCA is different from that in individuals with MODY3, it also supports the hypothesis that *HNF1A* mutations in HCA arise because of a genotoxic mechanism. First, we observed a consistent hotspot mutation at the codon 206 of *HNF1A* in HCA. Hotspots of transversion identified in tumors without a repeated nucleotide sequence context were previously suggested to be a hallmark of an exposure to a genotoxic compound, such as an R249S mutation in the *TP53* gene in hepatocellular carcinoma (HCC) associated with an exposure to the aflatoxin B1 mycotoxin (36,37).

Second, Hainaut and Pfeifer (26) showed that there is a significant difference in the pattern of TP53 mutations in lung cancers between smokers and nonsmokers, with a 30% frequency of G-to-T transversions in smoking-related lung cancer vs. 10% in non-smoking–related lung cancer. The overabundance of G-to-T transversions in smoking-related lung cancers was consistent with the studies of DNA damage and mutations due to benzo[*a*]pyrene and other cigarette smoke-derived carcinogens and their metabolites (38,39). Our observation of an uneven distribution among *HNF1A* nucleotide substitutions in HCA and high frequency of G-to-T transversions is in many ways similar to that in lung cancer caused by tobacco (Fig. 4*A*).

Third, Denissenko et al. (40) showed that the repair of benzo[*a*]pyrene diol epoxide adducts in the nontranscribed strand was slower than that in the transcribed strand and may explain the strand bias of transversions in cancer. Similarly, we observed that G-to-T transversions were significantly localized to the nontranscribed strand in H-HCA, an additional argument in favor of a genotoxic effect and, possibly, a presence of bulky DNA adducts.

Finally, the origin of such a genotoxic signature remains to be elucidated. We can hypothesize that it could be related to a particular genetic susceptibility and/or to an exposure to a specific toxic. According to the first hypothesis, we searched for mutations in *OGG1* and *MYH*, both genes specifically involved in the repair of 8-hydroxyguanine, a product of oxidative DNA damage that can also lead to G-to-T transversions (30–32). However, we did not observe mutations in these genes in patients with HCAs. In addition, we did not observe a higher level of oxidative stress in the livers of patients with a H-HCA. These results strongly suggest that exposure to an environmental agent appears to be the most likely event to explain the elevated rate of G-to-T transversions in H-HCA. Because HCA occurrence is highly associated with oral contraception, we can hypothesize that estrogen exposure could play a role in this mechanism. This last hypothesis is supported by the facts that *1*) the genotoxic activity of estrogen metabolites has been shown, particularly for catechol estrogens that may be oxidized to a reactive quinone capable of direct formation of DNA adducts (41,42); and *2*) germline heterozygous mutations of *CYP1B1*, a key metabolism enzyme responsible for the formation of hydroxylated and genotoxic metabolites of estrogen, contribute to the development of H-HCA in women using hormonal contraception (13).

In conclusion, when analyzing a large series of individuals with HCAs, we observed a significant differences between *HNF1A* somatic mutations identified in those with HCAs and the germline mutations identified in individuals with MODY3. Somatic mutations in HCA predict a more inactivating profile, resulting in a complete loss of function of the protein when biallelic. Moreover, we showed that the origin of the mutations might be the result of DNA damage caused by a genotoxic agent, possibly resulting from the metabolism of estrogen that could also be associated with a genetic susceptibility that remains to be identified.

ACKNOWLEDGMENTS

This work was supported in part by Institut National de la Santé et de la Recherche Médicale (INSERM) (Réseau de Recherche Clinique et en santé des populations), the Association pour la Recherche sur le Cancer (ARC), and the National Institutes of Health (R01-AA-16258 and R01-ES-15241). E.J. was supported by an ARC doctoral fellowship and J.Z.-R. by a "contrat d'interface" between INSERM and CHU Bordeaux.

No potential conflicts of interest relevant to this article were reported.

We thank all the participants of the Groupe d'étude Génétique des Tumeurs Hépatiques network. We are grateful to Sandra Rebouissou for helpful scientific discussion and critical reading of the manuscript.

REFERENCES

1. Baum JK, Bookstein JJ, Holtz F, Klein EW. Possible association between benign hepatomas and oral contraceptives. Lancet 1973;2:926–929

2. Edmondson HA, Reynolds TB, Henderson B, Benton B. Regression of liver cell adenomas associated with oral contraceptives. Ann Intern Med 1977;86:180–182
3. Flejou JF, Barge J, Menu Y, Degott C, Bismuth H, Potet F, Benhamou JP. Liver adenomatosis. An entity distinct from liver adenoma? Gastroenterology 1985;89:1132–1138
4. Bioulac-Sage P, Rebouissou S, Thomas C, Blanc JF, Saric J, Sa Cunha A, Rullier A, Cubel G, Couchy G, Imbeaud S, Balabaud C, Zucman-Rossi J. Hepatocellular adenoma subtype classification using molecular markers and immunohistochemistry. Hepatology 2007;46:740–748
5. Bluteau O, Jeannot E, Bioulac-Sage P, Marqués JM, Blanc JF, Bui H, Beaudoin JC, Franco D, Balabaud C, Laurent-Puig P, Zucman-Rossi J. Bi-allelic inactivation of TCF1 in hepatic adenomas. Nat Genet 2002;32:312–315
6. Rebouissou S, Amessou M, Couchy G, Poussin K, Imbeaud S, Pilati C, Izard T, Balabaud C, Bioulac-Sage P, Zucman-Rossi J. Frequent in-frame somatic deletions activate gp130 in inflammatory hepatocellular tumours. Nature 2009;457:200–204
7. Torbenson M, Lee JH, Choti M, Gage W, Abraham SC, Montgomery E, Boitnott J, Wu TT. Hepatic adenomas: analysis of sex steroid receptor status and the Wnt signaling pathway. Mod Pathol 2002;15:189–196
8. Zucman-Rossi J, Jeannot E, Nhieu JT, Scoazec JY, Guettier C, Rebouissou S, Bacq Y, Leteurtre E, Paradis V, Michalak S, Wendum D, Chiche L, Fabre M, Mellottee L, Laurent C, Partensky C, Castaing D, Zafrani ES, Laurent-Puig P, Balabaud C, Bioulac-Sage P. Genotype-phenotype correlation in hepatocellular adenoma: new classification and relationship with HCC. Hepatology 2006;43:515–524
9. Rebouissou S, Imbeaud S, Balabaud C, Boulanger V, Bertrand-Michel J, Tercé F, Auffray C, Bioulac-Sage P, Zucman-Rossi J. HNF1α inactivation promotes lipogenesis in human hepatocellular adenoma independently of SREBP-1 and carbohydrate-response element-binding protein (ChREBP) activation. J Biol Chem 2007;282:14437–14446
10. Yamagata K, Oda N, Kaisaki PJ, Menzel S, Furuta H, Vaxillaire M, Southam L, Cox RD, Lathrop GM, Boriraj VV, Chen X, Cox NJ, Oda Y, Yano H, Le Beau MM, Yamada S, Nishigori H, Takeda J, Fajans SS, Hattersley AT, Iwasaki N, Hansen T, Pedersen O, Polonsky KS, Turner RC, Velho G, Chèvre JC, Froguel P, Bell GI. Mutations in the hepatocyte nuclear factor-1α gene in maturity-onset diabetes of the young (MODY3). Nature 1996;384:455–458
11. Bacq Y, Jacquemin E, Balabaud C, Jeannot E, Scotto B, Branchereau S, Laurent C, Bourlier P, Pariente D, de Muret A, Fabre M, Bioulac-Sage P, Zucman-Rossi J. Familial liver adenomatosis associated with hepatocyte nuclear factor 1α inactivation. Gastroenterology 2003;125:1470–1475
12. Reznik Y, Dao T, Coutant R, Chiche L, Jeannot E, Clauin S, Rousselot P, Fabre M, Oberti F, Fatome A, Zucman-Rossi J, Bellanne-Chantelot C. Hepatocyte nuclear factor-1α gene inactivation: cosegregation between liver adenomatosis and diabetes phenotypes in two maturity-onset diabetes of the young (MODY)3 families. J Clin Endocrinol Metab 2004;89:1476–1480
13. Jeannot E, Poussin K, Chiche L, Bacq Y, Sturm N, Scoazec JY, Buffet C, Van Nhieu JT, Bellanné-Chantelot C, de Toma C, Laurent-Puig P, Bioulac-Sage P, Zucman-Rossi J. Association of CYP1B1 germ line mutations with hepatocyte nuclear factor 1α-mutated hepatocellular adenoma. Cancer Res 2007;67:2611–2616
14. Mendel DB, Hansen LP, Graves MK, Conley PB, Crabtree GR. HNF-1α and HNF-1β (vHNF-1) share dimerization and homeo domains, but not activation domains, and form heterodimers in vitro. Genes Dev 1991;5:1042–1056
15. Vaxillaire M, Abderrahmani A, Boutin P, Bailleul B, Froguel P, Yaniv M, Pontoglio M. Anatomy of a homeoprotein revealed by the analysis of human MODY3 mutations. J Biol Chem 1999;274:35639–35646
16. Akiyama TE, Ward JM, Gonzalez FJ. Regulation of the liver fatty acid-binding protein gene by hepatocyte nuclear factor 1α (HNF1α). Alterations in fatty acid homeostasis in HNF1α-deficient mice. J Biol Chem 2000;275:27117–27122
17. Hiraiwa H, Pan CJ, Lin B, Akiyama TE, Gonzalez FJ, Chou JY. A molecular link between the common phenotypes of type 1 glycogen storage disease and HNF1α-null mice. J Biol Chem 2001;276:7963–7967
18. Ishii Y, Hansen AJ, Mackenzie PI. Octamer transcription factor-1 enhances hepatic nuclear factor-1alpha-mediated activation of the human UDP glucuronosyltransferase 2B7 promoter. Mol Pharmacol 2000;57:940–947
19. Shih DQ, Bussen M, Sehayek E, Ananthanarayanan M, Shneider BL, Suchy FJ, Shefer S, Bollileni JS, Gonzalez FJ, Breslow JL, Stoffel M. Hepatocyte nuclear factor-1α is an essential regulator of bile acid and plasma cholesterol metabolism. Nat Genet 2001;27:375–382
20. Chi YI, Frantz JD, Oh BC, Hansen L, Dhe-Paganon S, Shoelson SE. Diabetes mutations delineate an atypical POU domain in HNF-1α. Mol Cell 2002;10:1129–1137
21. Bellanné-Chantelot C, Carette C, Riveline JP, Valéro R, Gautier JF, Larger E, Reznik Y, Ducluzeau PH, Sola A, Hartemann-Heurtier A, Lecomte P, Chaillous L, Laloi-Michelin M, Wilhem JM, Cuny P, Duron F, Guerci B, Jeandidier N, Mosnier-Pudar H, Assayag M, Dubois-Laforgue D, Velho G, Timsit J. The type and the position of HNF1A mutation modulate age at diagnosis of diabetes in patients with maturity-onset diabetes of the young (MODY)-3. Diabetes 2008;57:503–508
22. Harries LW, Ellard S, Stride A, Morgan NG, Hattersley AT. Isomers of the TCF1 gene encoding hepatocyte nuclear factor-1α show differential expression in the pancreas and define the relationship between mutation position and clinical phenotype in monogenic diabetes. Hum Mol Genet 2006;15:2216–2224
23. Rebouissou S, Vasiliu V, Thomas C, Bellanné-Chantelot C, Bui H, Chrétien Y, Timsit J, Rosty C, Laurent-Puig P, Chauveau D, Zucman-Rossi J. Germline hepatocyte nuclear factor 1α and 1β mutations in renal cell carcinomas. Hum Mol Genet 2005;14:603–614
24. Livak KJ, Schmittgen TD. Analysis of relative gene expression data using real-time quantitative PCR and the $2(^{-\Delta\Delta C_T})$ method. Methods 2001;25:402–408
25. Ellard S, Colclough K. Mutations in the genes encoding the transcription factors hepatocyte nuclear factor 1α (HNF1A) and 4α (HNF4A) in maturity-onset diabetes of the young. Hum Mutat 2006;27:854–869
26. Hainaut P, Pfeifer GP. Patterns of p53 G→T transversions in lung cancers reflect the primary mutagenic signature of DNA-damage by tobacco smoke. Carcinogenesis 2001;22:367–374
27. Denissenko MF, Pao A, Tang M, Pfeifer GP. Preferential formation of benzo[a]pyrene adducts at lung cancer mutational hotspots in P53. Science 1996;274:430–432
28. Michaels ML, Miller JH. The GO system protects organisms from the mutagenic effect of the spontaneous lesion 8-hydroxyguanine (7,8-dihydro-8-oxoguanine). J Bacteriol 1992;174:6321–6325
29. Rusyn I, Asakura S, Pachkowski B, Bradford BU, Denissenko MF, Peters JM, Holland SM, Reddy JK, Cunningham ML, Swenberg JA. Expression of base excision DNA repair genes is a sensitive biomarker for in vivo detection of chemical-induced chronic oxidative stress: identification of the molecular source of radicals responsible for DNA damage by peroxisome proliferators. Cancer Res 2004;64:1050–1057
30. Al-Tassan N, Chmiel NH, Maynard J, Fleming N, Livingston AL, Williams GT, Hodges AK, Davies DR, David SS, Sampson JR, Cheadle JP. Inherited variants of MYH associated with somatic G:C→T:A mutations in colorectal tumors. Nat Genet 2002;30:227–232
31. Audebert M, Chevillard S, Levalois C, Gyapay G, Vieillefond A, Klijanienko J, Vielh P, El Naggar AK, Oudard S, Boiteux S, Radicella JP. Alterations of the DNA repair gene OGG1 in human clear cell carcinomas of the kidney. Cancer Res 2000;60:4740–4744
32. Slupska MM, Baikalov C, Luther WM, Chiang JH, Wei YF, Miller JH. Cloning and sequencing a human homolog (hMYH) of the *Escherichia coli* mutY gene whose function is required for the repair of oxidative DNA damage. J Bacteriol 1996;178:3885–3892
33. Byers PH. Killing the messenger: new insights into nonsense-mediated mRNA decay. J Clin Invest 2002;109:3–6
34. Frischmeyer PA, Dietz HC. Nonsense-mediated mRNA decay in health and disease. Hum Mol Genet 1999;8:1893–1900
35. Harries LW, Hattersley AT, Ellard S. Messenger RNA transcripts of the hepatocyte nuclear factor-1α gene containing premature termination codons are subject to nonsense-mediated decay. Diabetes 2004;53:500–504
36. Bressac B, Kew M, Wands J, Ozturk M. Selective G to T mutations of p53 gene in hepatocellular carcinoma from southern Africa. Nature 1991;350:429–431
37. Hsu IC, Metcalf RA, Sun T, Welsh JA, Wang NJ, Harris CC. Mutational hotspot in the p53 gene in human hepatocellular carcinomas. Nature 1991;350:427–428
38. Greenblatt MS, Bennett WP, Hollstein M, Harris CC. Mutations in the p53 tumor suppressor gene: clues to cancer etiology and molecular pathogenesis. Cancer Res 1994;54:4855–4878
39. Hollstein M, Sidransky D, Vogelstein B, Harris CC. p53 mutations in human cancers. Science 1991;253:49–53
40. Denissenko MF, Pao A, Pfeifer GP, Tang M. Slow repair of bulky DNA adducts along the nontranscribed strand of the human p53 gene may explain the strand bias of transversion mutations in cancers. Oncogene 1998;16:1241–1247
41. Cavalieri EL, Stack DE, Devanesan PD, Todorovic R, Dwivedy I, Higginbotham S, Johansson SL, Patil KD, Gross ML, Gooden JK, Ramanathan R, Cerny RL, Rogan EG. Molecular origin of cancer: catechol estrogen-3,4-quinones as endogenous tumor initiators. Proc Natl Acad Sci U S A 1997;94:10937–10942
42. Yager JD, Liehr JG. Molecular mechanisms of estrogen carcinogenesis. Annu Rev Pharmacol Toxicol 1996;36:203–232